Int. J. Plasma Environ. Sci. Technol. 17 (2023) e01007 (12pp)

International Journal of Plasma Environmental Science and Technology

Regular Paper

DOI: 10.34343/ijpest.2023.17.e01007

CO_2 conversion characteristics by micro-gap DBD plasma reactor

Yukio Hayakawa*, Primas Emeraldi, Tsutomu Imai, Shinji Kambara

Environmental and Renewable Energy System Division, Graduate School of Engineering, Gifu University, Japan

* Corresponding author: hayakawa.yukio.j4@f.gifu-u.ac.jp (Yukio Hayakawa)

Received: 15 December 2022
Revised: 29 March 2023
Accepted: 29 March 2023
Published online: 3 April 2023

Abstract

CO_2 conversion into CO and O_2 using dielectric barrier discharge (DBD) reactors suffers from a low conversion and energy efficiency. Therefore, proper tuning of plasma processing parameters and modification of DBD reactor design is needed to enhance the CO_2 conversion performance. This study investigated the combined effect of micro-gap discharge and pulsed power on the CO_2 conversion performance of the pure CO_2 splitting process. The CO_2 conversion, energy efficiency and CO selectivity were evaluated at various discharge power and gas flow rate. Moreover, the electrical characterization was performed to evaluate the effect of these processing parameters on the plasma regime of the pulsed micro-gap DBD reactor. The findings indicate that the CO_2 conversion and streamer intensity were significantly influenced by gas flow rate, while the energy efficiency and discharge regime were greatly affected by discharge power. All the decomposed CO_2 was also decomposed into CO and O_2. The maximum CO_2 conversion of 51.42% was obtained at an SEI of 154.74 kJ L^{-1} with a corresponding energy efficiency of 4.15%. On the other hand, the highest energy efficiency of 9.43% was achieved at an SEI of 25.26 kJ L^{-1} with a corresponding CO_2 conversion of 4.15%. Most of the decomposed CO_2 was converted to CO and O_2, but small amounts of carbon precipitation were also observed under low flow conditions. These results suggest that the pulsed micro-gap DBD might be more favorable than the DBD reactor with expensive packing material for industrial application.

Keywords: Non-thermal plasma, CO_2 conversion, dielectric barrier discharge, micro-gap reactor.

1. Introduction

Carbon dioxide (CO_2), the most abundant greenhouse gas emitted by human activity, is a major contributor to climate change in modern society [1]. This increase in global temperature poses a serious threat to the natural environment and humanity. Therefore, it is necessary to try to use the emitted CO_2 as a natural carbon source capable of producing synthesis gases and value-added chemicals [2]. Using CO_2 as a carbon source is an attractive alternative for the traditional fossil industry [3]. Several methods of CO_2 utilization have been proposed using renewable energy source in practice [4].

One of the promising approaches to sustainably reduce CO_2 emission is Carbon capture and utilization (CCU). CCU involves capturing the CO_2 from an emission source like industrial processes and power plants and using the captured CO_2 as a feedstock to produce syngas [5]. The CO_2 splitting into CO is an interesting CCU route as CO is an essential chemical feedstock for the Fischer-Tropsch process, producing liquid hydrocarbons, synthetic petroleum, and oxygenates [6]. This route, thus, provides an effective solution for the greenhouse gas problem by transforming CO_2 into a valuable energy resource.

However, CO_2 splitting in traditional thermal processes (Eq. (1)) requires a large amount of energy since CO_2 is a highly stable molecule [7]. The previous thermodynamic analysis demonstrates that CO_2 splitting requires a temperature around 3600 K [8]. Moreover, the thermal decomposition of CO_2 also suffers from high energy costs since a considerable amount of energy is lost in heating the entire gas. Therefore, a more efficient CO_2 splitting method is required for a viable CCU process.

$$CO_2 \rightarrow CO + \frac{1}{2}O_2 \quad \Delta H = 128 kJ/mol\ (2.93\ eV) \tag{1}$$

Non-thermal plasma (NTP) technology provides an alternative way to decompose CO_2, which accommodates CO_2 activation at a lower temperature [9]. The gas temperature in non-thermal plasmas can be as low as room temperature. At the same time, the electrons are accelerated by the applied electric field with an average energy of 1–10 eV, which can activate the gas by electron impact excitation, ionization, and dissociation [10]. In addition, due to its instant start-up and switch-off, NTP CO_2 decomposition can serve as a potential chemical energy storage for the surplus electricity from renewable energy during the peak periods, leading to a significant decrease in the overall energy cost for the CO_2 decomposition process [11, 12]. Various NTP systems have been proposed for the direct conversion of CO_2, including dielectric barrier discharge (DBD) [13–19], gliding arc discharge [20, 21], corona discharge [22], microwave discharge [23, 24], and glow discharge [25].

In recent years, DBD reactors have become available with mild operating conditions (near atmospheric pressure and room temperature), simple design, and easy upscaling to industrial applications, with potential applications in CO_2 to CO and O_2 conversion devices [26]. In addition, DBD plasma systems can be easily filled with packing materials (simple dielectric beads or catalysts), providing additional improvements in CO_2 dissociation reactions [27]. In terms of CO_2 conversion performance, the process parameters of the DBD reactor play an important role. Plasma process parameters strongly influence CO_2 conversion and energy efficiency [13–16, 28, 29]. These plasma process parameters include discharge power, discharge gap, dielectric material properties, and gas flow rate.

The ratio of the discharge power to the gas flow rate (i.e., Specific Energy Input (SEI)) is the most dominant factor determining the conversion and energy efficiency of CO_2 splitting using DBD plasma reactors. Aerts *et al*. [14] demonstrate that proper tuning of discharge power versus gas flow rate can increase the conversion and energy efficiency at certain SEI. However, the main downside of CO_2 conversion using DBD plasma is its low energy efficiency and the trade-off between CO_2 conversion and energy efficiency [9,30]. This is because DBD generally operate under high reduced electric field conditions. Under high reduced electric field conditions, most of the energy is spent on electron impact excitation of CO_2, but CO_2 decomposition by electron impact excitation is not energy efficient. Therefore, there is a trade-off between CO_2 decomposition rate and energy efficiency. For example, Alliati *et al*. [30] reported a maximum CO_2 conversion rate is up to 22.4 % with only 2.1 % energy efficiency, but when the CO_2 conversion rate decreased to 17.4 %, the energy efficiency was up to 8.3 %. Therefore, a practical industrial application of DBD plasma CO_2 conversion requires further modification to enhance the CO_2 conversion and energy efficiency.

The modification of the DBD reactor design could increase CO_2 conversion and energy efficiency. Mei *et al*. [31] proposed a DBD reactor with an aluminum foil outer electrode and stainless-steel screw-type inner electrode. Their experimental results demonstrated the enhanced local electric field near the sharp edges of the inner electrode and the enlarged effective area of the outer electrode that gives rise to CO_2 conversion and energy efficiency. Another practical way to enhance the electric field in the DBD reactor is by reducing the discharge gap up to the micrometer range. This method provides a more uniform discharge, thus significantly increasing the CO_2 conversion [32]. In fact, micro-gap plasma reactors are highly effective in gas processing. For example, Younas *et al.* have succeeded in significantly reducing the energy efficiency of hydrogen production from water vapor by using micro plasma reactors [33]. Wang *et al*. also reported that the conversion rate of methane reforming can be improved by converting a conventional plasma reactor to a micro-gap plasma reactor [34]. However, this higher CO_2 conversion comes at high SEI, consequently low energy efficiency. The energy efficiency can be further improved by utilizing pulsed power instead of alternating current (AC) power commonly used in conventional DBD reactors. Pulsed power inhibits overheating of the gas while enhancing the stability of discharge and altering the plasma regime, thus providing a more efficient CO_2 conversion process [35, 36]. Dimas *et al*. have already investigated the behavior of CO_2 decomposition using a high frequency AC power source and a micro-gap plasma reactor [37]. In this paper, it is reported that the energy efficiency of CO_2 decomposition improves with shorter gap lengths under pressure conditions below atmospheric pressure, with a maximum energy efficiency obtained at a 0.5 mm gap in the 0.5-3.0 mm range. In addition, a high-frequency AC power supply was used, with a maximum energy efficiency of about 5%. Therefore, we focused on the possibility of combining micro-gap structure and pulsed power to simultaneously improve CO_2 conversion efficiency and energy efficiency.

In this study, we investigate the combined effect of micro-gap discharge and pulsed power on the CO_2 conversion performance of pure CO_2 splitting. The CO_2 conversion, energy efficiency, CO selectivity, and CO yield were examined at a variety of discharge power and gas flow rate. In addition, the electrical characterization was performed to evaluate the effect of discharge power and gas flow rate on the plasma regime of the pulsed micro-gap DBD reactor. At last, the CO_2 conversion and energy efficiency were compared with other literature studies on DBD CO_2 decomposition.

2. Experimental

2.1 Experimental setup for CO_2 decomposition

Fig. 1 illustrates the schematic diagram of the experimental setup for CO_2 decomposition by impulse DBD plasma. The apparatus included a tubular DBD plasma reactor, an impulse high voltage power supply, an electrical measurement system, a gas supply system, and a gas analysis section. The plasma reactor consists of a dielectric tube and two concentric cylindrical electrodes. A quartz tube with an outer diameter of 45.3 mm and a wall thickness of 2 mm was used as a dielectric barrier. The inner electrode was a stainless-steel rod with an outer diameter of 40.8 mm placed in the center of the quartz tube and fixed by two o-rings. The stainless-steel rod was equipped with holes at both ends that serve as gas inlet and outlet. A 100 mm long stainless-steel foil was wrapped around the quartz tube (ε = 3.5~3.8) as an outer electrode. The reactor configuration provided a fixed discharge gap of 250 μm that is considered a micro-gap DBD reactor and a discharge volume of 3.22 mL. In a previous study [37], it was reported that the energy efficiency of CO_2 decomposition decreases inversely proportional to the gap length. Therefore, the gap length was set at 250 μm with reference to the limit of machining accuracy of quartz tube and electrode rod. The outer electrode was then connected to the impulse high voltage source, and the inner electrode was grounded. Therefore, the reactor was defined as a pulsed micro-gap DBD reactor.

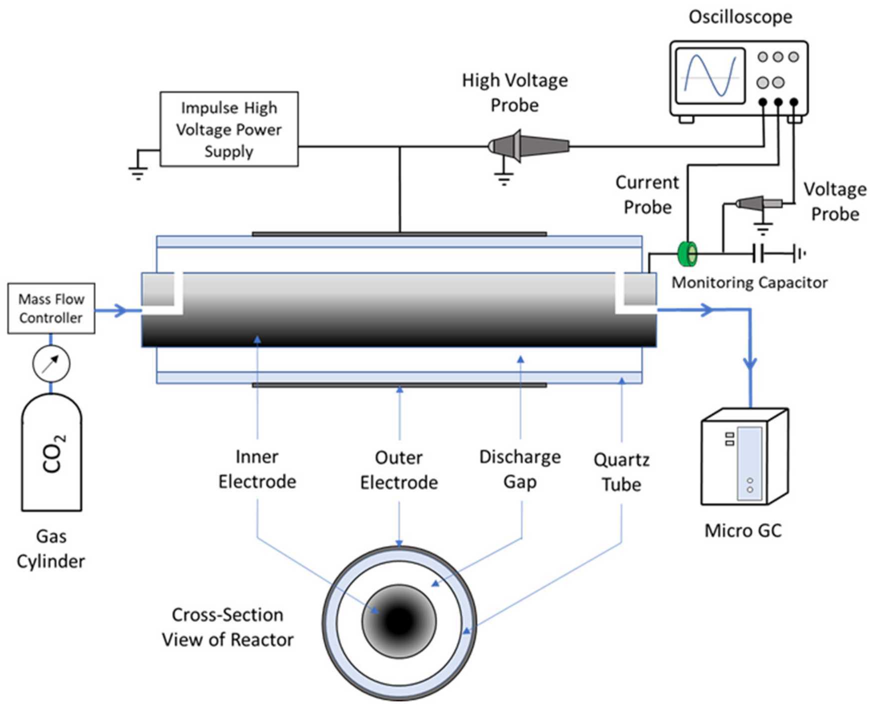

Fig. 1. Schematic diagram of the CO_2 decomposition experimental setup.

The gas circuit consisted of CO_2 supply, mass flow controller, and gas analysis device. On the other hand, the electrical system consisted of a power supply and electrical signal measuring devices. First, pure CO_2 (99.999%) gas was sent through the DBD reactor as the feed gas. The feed gas flow rate was controlled by mass flow controllers (Allicat) and was varied at 10, 20, 50 100 mL min^{-1}. After the gas passed through the DBD reactor, the gas composition was analyzed using a two-channel micro-gas chromatograph (Agilent

3000A Micro-GC). The micro-GC was equipped with two columns (molecular Sieve 5 A and Poraplot Q column) and a thermal conductivity detector (TCD) on each channel. The molecular Sieve 5 A column allowed the identification of CO and O_2 gas concentrations, which were product gas, whereas the Poraplot Q column allowed the concentration of CO_2 to be determined.

After the sample gas flow rate into the reactor was maintained, a plasma discharge was then ignited by an impulse high voltage power supply (PHF-2KL, Haiden). The supply voltage was varied at 12, 14, 16 to 18 $kV_{p\text{-}p}$ at a constant frequency of 10 kHz. Then, the applied voltage (V(t)) and the total current (I(t)) were measured by a high voltage probe (Tektronix, P6015A) and a current probe (Pearson, 2887), respectively. The pulsed power waveforms obtained from the measured voltage and current were shown in Fig. 2. Besides, the charge (Q) generated by plasma discharge was determined using a measuring capacitor (26.4 nF) placed between the inner electrode and ground and was measured by a voltage probe (Tektronix, P2220). Finally, all the electrical signals were recorded using a four-channel digital oscilloscope (Tektronix, DPO3034).

Note that each discharge electric signal and associated gas products measurement was carried out after the reactor wall temperature became stable to ensure that plasma discharge had reached a steady-state condition. The reactor wall temperature was monitored by a thermal infrared camera (FLIR). Furthermore, each experimental condition was performed with a clean inner electrode and reactor wall to ensure experimental consistency. Finally, all measurements were repeated at least three times, and an average result and standard error were used.

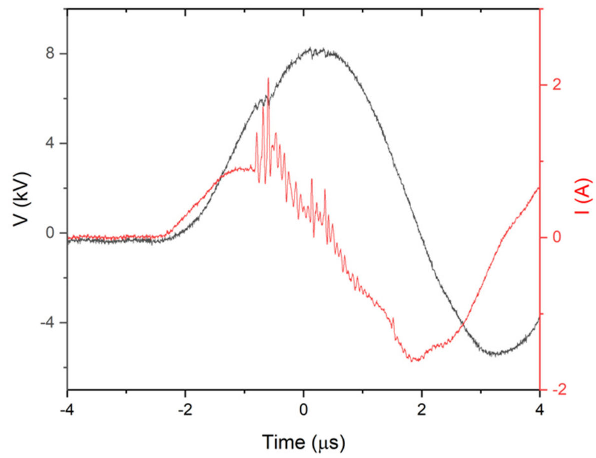

Fig. 2. Voltage-current waveform of the pulsed micro-gap DBD reactor. Applied voltage: 14 $kV_{p\text{-}p}$.

2.2 CO_2 conversion performance characterization

The CO_2 conversion performance parameters, including CO_2 conversion rate, specific energy input, energy efficiency was calculated based on the assumption that CO_2 decomposition occurred through an electron impact dissociation reaction. This reaction produces only CO and O_2 (Eq. 1). In this regard, the CO_2 conversion was calculated from micro-GC measurement data as follows:

$$X_{GC}[\%] = \left(\frac{CO_{2,in} - CO_{2,out}}{CO_{2,out}}\right) \times 100\% \tag{2}$$

where $CO_{2,in}$ and $CO_{2,out}$ represent the concentration of CO_2 at the inlet and outlet of the reactor, respectively. However, this conversion value is incorrect because the expansion effect caused by splitting one mole of CO_2 into one mole of CO and 0.5 mole of O_2 gives rise to a gas expansion, thus overestimating the conversion value. Consequently, the overestimated value was corrected to get the actual CO_2 conversion (X_{CO2}) by the following equation [38]:

$$X_{CO2}[\%] = \left(\frac{2X_{GC}}{3 - X_{GC}}\right) \times 100\% \tag{3}$$

The ratio of the plasma discharge power to the gas feed flow rate, also known as specific energy input (SEI), was calculated as:

$$\text{SEI}\left[\text{kJ L}^{-1}\right] = \frac{Power[W]}{Flow\ rate[mL\ min^{-1}]} \times 60\ [s/min] \quad (4)$$

The energy efficiency (η) was then determined by:

$$\eta[\%] = \frac{\Delta H_R[kJ\ mol^{-1}]\ X_{CO2}[\%]}{SEI[kJ\ L^{-1}]\ V_m\ [L\ mol^{-1}]} \quad (5)$$

where ΔH_R is the reaction enthalpy of pure CO_2 splitting at the temperature of 298°K (283.3 kJ mol^{-1}), and V_m is the molar gas volume (22.4 L mol^{-1}). Note that the enthalpy value of the CO_2 splitting reaction is stable in the range of temperature from 298 to 473 K (i.e., the typical gas temperature of the DBD plasma) [39]. Finally, the CO selectivity (S_{CO}) was defined as follow:

$$S_{CO}[\%] = \frac{CO_{out}}{CO_{2,in} - CO_{2,out}} \times 100 \quad (6)$$

2.3 Electrical characterization

The signals recorded by oscilloscope were analyzed to determine the electrical characteristics of the discharge, such as discharge power, gap voltage (U_g), and discharge current (I_g). The discharge power was calculated from the area of the Q-V plot multiplied by the frequency (1/T), known as the Lissajous figure method [40], expressed by Eq. (7).

$$P = \frac{1}{T} \oint_0^T Q(V)dV \quad (7)$$

Based on its electrical characteristic, the DBD reactor behaves as a capacitor (C_{cell}) that can be represented as a serial connection of the dielectric barrier capacitance (C_d) and gas gap capacitance (C_g) and can be expressed as in Eq. (8). The values of C_{cell} and C_d were determined using the method proposed by Pipa *et al.* [41], which gives an accurate value of the effective capacitances for pulsed driven DBD. For the micro-gap plasma reactors in this study, C_d = 296.7 pF, C_g=259.4 pF, and C_{cell} = 138.4 pF.

$$C_{cell} = \frac{C_d C_g}{C_d + C_g} \quad (8)$$

These capacitances values, along with the measured applied voltage ($V(t)$) and the total current ($I(t)$), were then applied to calculate the gas gap voltage ($U_g(t)$) and discharge current ($I_g(t)$) based on the equivalent circuit of the coaxial DBD reactor according to Eq. (9) and Eq. (10), respectively [42]. The calculated voltage gap and discharge current waveform were used to evaluate the plasma regime inside the reactor during the variation of discharge power and gas flow rate.

$$U_g(t) = V(t) - \frac{Q(t)}{C_d} \quad (9)$$

$$I_g(t) = \frac{1}{1 - \frac{C_{cell}}{C_d}}\left[I(t) - C_{cell}\frac{dV(t)}{dt}\right] \quad (10)$$

3. Results and discussion

3.1 CO_2 conversion characteristics of micro-gap DBD reactor

Fig. 3 shows the influence of discharge power on the CO_2 conversion and energy efficiency for a gas flow rate of 100 mL min^{-1}. The discharge power was calculated from the measured values of the applied voltage and discharge current and the pulse frequency. It is apparent from this figure that there was a trade-off between CO_2 conversion and energy efficiency. For example, as the discharge power changed from 34.48 to 101.13 W, CO_2 conversion increased from 10.17 to 20.25%. On the other hand, energy efficiency decreased from 6.47 to 4.17%. It has been observed that almost all the decomposed CO_2 is broken down into CO and O_2 by GC analysis.

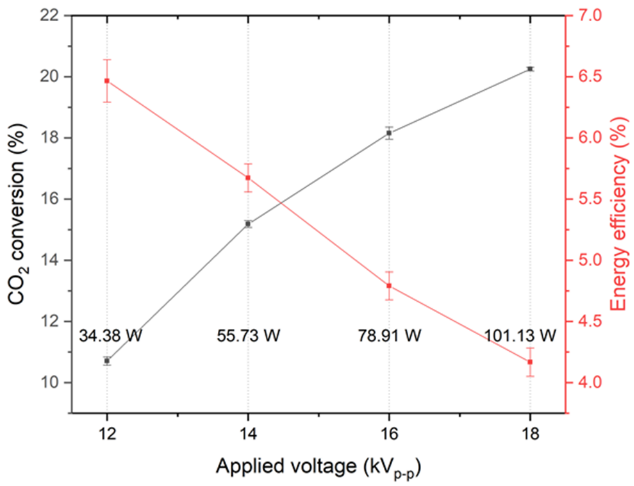

Fig. 3. Conversion and energy efficiency for different discharge power at a gas flow rate of 100 mL min^{-1}.

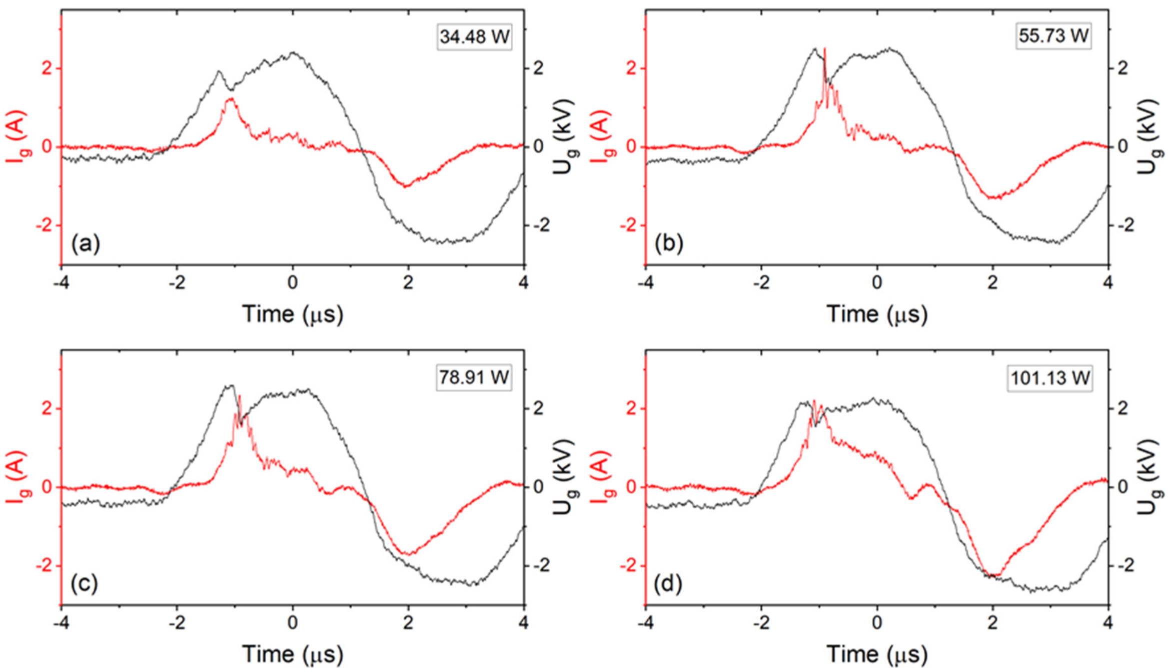

Fig. 4. Gap voltage and discharge current waveform of a) 34.48 W, b) 55.73 W, c) 78.91 W, and d) 101.13 W at gas flow rate of 100 mL min^{-1}.

In addition, the level of discharge power (i.e., the applied voltage) strongly affected the electrical characteristic of the reactor. As shown in Fig. 4, increasing the applied voltage from 12 $kV_{p\text{-}p}$ to 18 $kV_{p\text{-}p}$ increased both the peak-to-peak value of the gap voltage and discharge current, which may contribute to the enhanced CO_2 conversion. Interestingly, variation of discharge power produced different plasma behavior. In the case of discharge power of 34.48 W, no streamer formation was observed from the discharge current waveform (Fig. 4 (a)), indicating the discharge is in uniform mode. This discharge behavior differs from CO_2 plasma using a conventional millimeter-gap DBD reactor supplied with AC voltage [13, 16, 43] and a micro-gap DBD supplied with AC voltage [32], which is developed a filamentary behavior. Moreover, the discharge current peak was significantly higher than the current peak on filamentary discharge.

Interestingly, increasing the discharge power to 55.73 W produced a streamer with a higher peak value. Although only a single streamer formation was generated during a total period of pulse voltage (Fig. 4 (b)), this streamer demonstrates a change in the discharge regime from a uniform mode to a combination of uniform mode and filamentary mode. Moreover, discharge current with a higher peak indicates a higher electrons and ions density, resulting in more reactive plasma [15,30]. However, the further increase in the discharge power did not expand the streamer formation. This finding contrasts with previous studies on CO_2 decomposition using a millimeter-gap DBD reactor supplied with AC voltage [31], which demonstrated the increasing streamer intensity with increased discharge power.

Moreover, the peak value of discharge current at discharge power of 78.91 and 101.13 W was lower than in the case of 55.73 W. The different behavior of the streamer might be due to significant differences in discharge gap length and voltage supply waveform used in this present study, resulting in a completely different electric field configuration and discharge mode. Nevertheless, it is interesting to note that the discharge power strongly affects the plasma regime of the pulsed micro-gap DBD reactor.

Fig. 5 shows the influence of the gas flow rate on the CO_2 conversion and energy efficiency at constant discharge power of 55 W. The decrease in gas flow rate extends the residence time of CO_2 gases in the plasma, which increases the probability of CO_2 dissociation through the electron impact reaction and collisions with active species, consequently enhancing the CO_2 conversion [14, 30, 31]. For example, reducing the flow rate from 100 to 20 mL min^{-1} lengthens the residence time from 1.93 to 9.67 s, which increases the CO_2 conversion from 15.19 to 51.42%. However, the residence time becomes too long at a flow rate of 10 mL min^{-1} (i.e., 19.33 s), leading to a high rate of backward reaction [14], thus decreasing the CO_2 conversion. On the other hand, the energy efficiency was increased from 1.79 to 7.25% by increasing the feed flow rate from 10 to 50 mL min^{-1}. However, increasing the gas flow rate to 100 mL min^{-1} reduces the energy efficiency due to a considerably low CO_2 conversion value.

Furthermore, the gas flow rate significantly affected the discharge current, as shown in Fig. 6. On the other hand, the gas flow rate showed a negligible effect of gap voltage. At a constant discharge power, a lower gas flow rate seems to increase the streamer intensity of the plasma discharge. The highest streamer intensity was found at the 20 mL min^{-1} gas flow rate, which corresponds to the maximum CO_2 conversion of 51.42%. Although the overall plasma regime exhibits a combination of the uniform mode and filamentary mode, this result indicates that streamer formation played a significant role in the CO_2 dissociation process on pulsed micro-gap DBD. Previous research reports indicate that most of the CO_2 decomposition by plasma is due to electron impact reactions, and it is thought that the electron impact reactions are further promoted by the generation of streamers [14, 30].

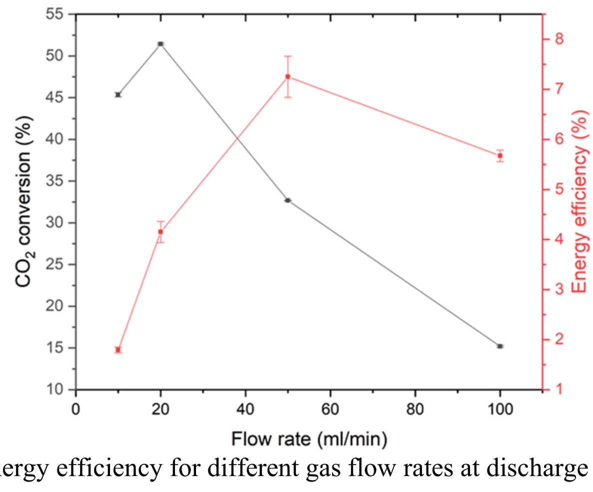

Fig. 5. Conversion and energy efficiency for different gas flow rates at discharge power of ≈ 50 W.

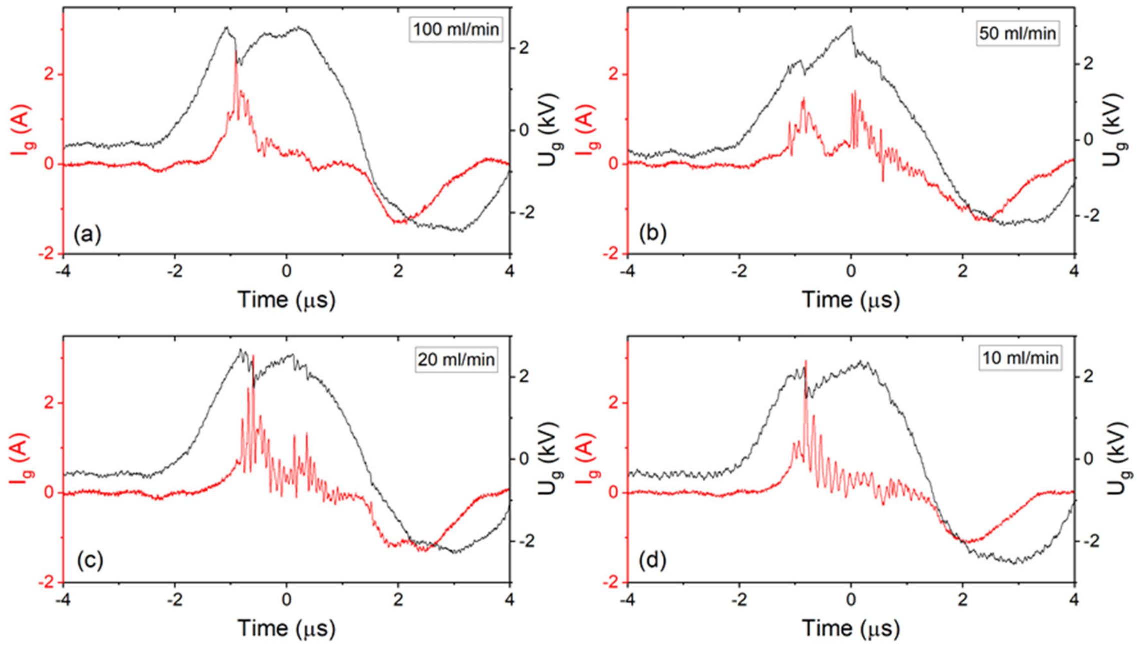

Fig. 6. Gap voltage and discharge current waveform for a gas flow rate of a) 100 mL min^{-1}, b) 50 mL min^{-1}, c) 20 mL min^{-1}, and d) 10 mL min^{-1} at discharge power of ≈ 55 W.

3.2 CO selectivity of micro-gap plasma reactor

The CO_2 decomposition process in DBD plasma is mainly conducted through electron impact dissociation, electron impact ionization, and electron dissociative attachment reaction, where CO and O_2 are the main product [9]. CO can be further dissociated into carbon and oxygen atom through CO dissociation by electron impact reaction during the CO_2 conversion process [43]. Therefore, the influence of discharge power and gas flow rate on CO selectivity was evaluated to determine the carbon balance from the CO_2 splitting process. Fig. 7 shows the influence of the applied voltage (i.e., discharge power) on CO selectivity at a different gas flow rate. CO selectivity was almost independent of discharge power. In the case of a 100 mL min^{-1} gas flow rate, the CO selectivity is close to 100%. This result suggests that stoichiometric conversion of CO_2 into CO was achieved at the gas flow rate of 100 mL min^{-1}. However, decreasing the gas flow rate to 20 mL min^{-1} reduced the CO selectivity to 79.98 %. Indeed, some carbon deposits were observed at the inner electrode and dielectric surface. Carbon deposition during the CO_2 splitting process was also found in previous studies, which is associated with a high discharge current peak resulting in high CO_2 conversion [44, 45]. Fig. 6 shows that the discharge current in the 20 mL min^{-1} flow rate condition is higher than in the other conditions. Therefore, the carbon formation reaction from CO is considered to have occurred, resulting in a decrease in CO selectivity.

3.3 Evaluation of SEI

The CO_2 conversion and energy efficiency are often presented as a function of SEI, which has been considered a major variable that determines the CO_2 conversion performance [9, 14]. Fig. 8 illustrates the effect of SEI for different values of discharge power and gas flow rate (i.e., residence time) on CO_2 conversion and energy efficiency. Note that the result for the gas flow rate of 10 mL min^{-1} was not included in Fig. 8 because it gave rise to a significantly high SEI without improvement in CO_2 conversion and energy efficiency.

The gas flow rate (i.e., residence time) seems to have a more pronounced effect on the conversion than the plasma power. For example, increasing SEI from 20.69 to 81.75 kJ L^{-1} by tuning the gas flow rate increases the CO_2 conversion from 10.71 to 43.31%. On the other hand, a relatively similar increase in SEI from 25.26 to 88.67 kJ L^{-1} by changing the discharge power results in a lower increase in CO_2 conversion from 19.08 to 37.52%. However, the plasma power appears to play a more critical role in determining the efficiency of the plasma
CO_2 conversion, as shown in Fig. 8. This behavior of SEI was also found in previous studies on CO_2 splitting using conventional cylindrical DBD reactor [14, 30] and modified cylindrical DBD reactor [31].

In addition, similar SEI values could produce different CO_2 conversion and energy efficiency. For example, an SEI value of 56.29 kJ L^{-1} from a combination of discharge power of 46.91 W and gas flow rate of 50 mL min^{-1} produced a higher CO_2 conversion and energy efficiency than an SEI value of 60.68 kJ L^{-1} from a combination of discharge power of 101.13 W and gas flow rate of 100 mL min^{-1}. This result corroborates a previous study that the conversion and energy efficiency at a certain SEI can be increased by tuning the plasma power and the gas flow rate [14]. The discharge current waveforms of these relatively similar SEI values are shown in Fig. 4 (b) and Fig. 6 (d), respectively. The combination of low discharge power and gas flow rate generated a higher streamer intensity (Fig. 4 (b)) than the combination of high discharge power and gas flow rate (Fig. 6 (d)). This result confirms the significant influence of streamer intensity on CO_2 conversion and energy efficiency of the pulsed micro-gap DBD reactor.

The results of this study indicate that the combined effect of micro-gap discharge and pulsed power appears to enhance the CO_2 conversion of the DBD reactor considerably. The maximum CO_2 conversion of 51.42% achieved in this study was significantly higher than in previous studies using conventional DBD reactor. Besides, the maximum energy efficiency of 9.43% was in the same order as the typical result for a DBD reactor. Table 1 compares the CO_2 conversion and energy efficiency of pure CO_2 decomposition using different DBD reactors. It should be noted that the CO_2 conversion of 53.7% from [32] was achieved at significantly high SEI, and the CO_2 conversion of 64.8% from [47] was produced on a DBD reactor with mixed packing material and equipped with a water-cooling system.

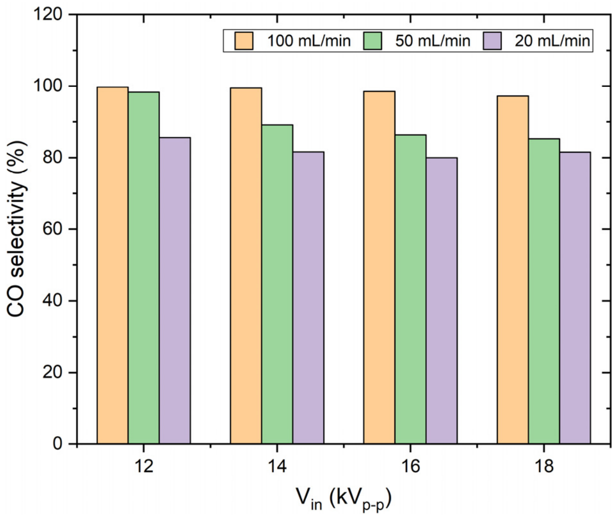

Fig. 7. CO selectivity at various applied voltage for gas flow rate of 20, 50, and 100 mL min^{-1}.

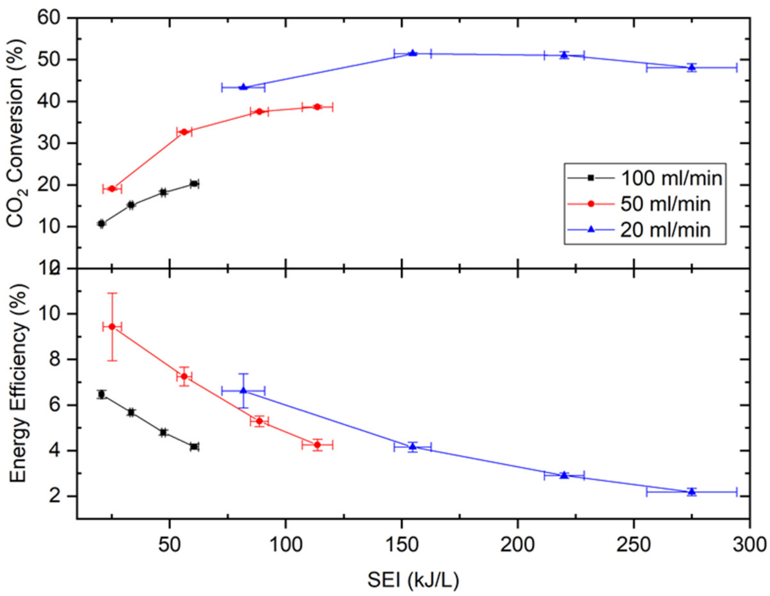

Fig. 8. CO_2 conversion and energy efficiency at different SEI values.

Table 1. Comparison of the CO_2 conversion and energy efficiency of pure CO_2 decomposition using different DBD reactors.

Reactor type	Discharge gap (mm)	Maximum CO_2 conversion SEI ($kJ\ L^{-1}$)	CO_2 conversion (%)	Energy efficiency (%)	Maximum energy efficiency SEI ($kJ\ L^{-1}$)	CO_2 conversion (%)	Energy efficiency (%)	Ref.
DBD	0.25	154.7	51.4	4.2	25.3	19.1	9.4	This study
DBD	2.50	120.0	27.0	2.8	24.0	20.0	10.4	[31]
DBD	1.80	229.0	35.0	2.0	25.0	3.1	8.0	[14]
DBD	0.70	60.0	18.0	1.7	20.6	9.6	3.8	[28]
DBD	0.30	602.0	53.7	1.1	156.3	33.3	2.7	[32]
PBDBD	No data	60.0	27.4	4.6	10.0	8.0	9.2	[48]
PBDBD	4.50	240.0	42.0	4.7	36.0	10.0	9.6	[19]
PBDBD	5.00	330.0	64.4	2.4	18.0	12.6	8.8	[47]

PBDBD: packed bed DBD

4. Conclusion

In this study, pure CO_2 splitting into CO and O_2 has been performed in a micro-gap DBD plasma reactor supplied by an impulse high voltage. Plasma operating conditions (i.e., discharge power and gas flow rate) controlled the plasma regime and residence time that determine the CO_2 decomposition performance (CO_2 conversion, energy efficiency). The findings of this study suggest that the CO_2 conversion and streamer intensity were significantly influenced by the gas flow rate. On the other hand, the energy efficiency and discharge regime seem to be strongly affected by the discharge power. The maximum CO_2 conversion of 51.42% was obtained at an SEI of 154.74 $kJ\ L^{-1}$ with a corresponding energy efficiency of 4.15%. On the other hand, the highest energy efficiency of 9.43 was achieved at an SEI of 25.26 $kJ\ L^{-1}$ with a corresponding CO_2 conversion of 19.08%. Most of the decomposed CO_2 was converted to CO and O_2. A small amount of carbon precipitation was also observed under low flow conditions due to enhanced streamer formation. These results seem to be comparable to the typical results from a packed-bed DBD reactor. Therefore, the pulsed micro-gap DBD might be more favorable than the DBD reactor with expensive packing material for industrial application.

Acknowledgment

This work was based on the tools of the technological platform supported by the project for technology development of carbon recycling, next-generation thermal power generation, etc. and technology development at the CO_2 effective utilization base by New Energy and Industrial Technology Development Organization (NEDO).

References

[1] Letcher T.M., Global warming—a complex situation, in: Climate Change, Elsevier, pp. 3–17, 2021.
[2] Sakakura T., Choi J.C., and Yasuda H., Transformation of carbon dioxide, *Chem. Rev.*, Vol. 107 (6), pp.2365–2387, 2007.
[3] Yang H., Zhang C., Gao P., Wang H., Li X., Zhong L., Wei W., and Sun Y., A review of the catalytic hydrogenation of carbon dioxide into value-added hydrocarbons., *Catal. Technol.*, Vol. 7, pp. 4580–4598, 2017.
[4] Centi G. and Perathoner S., Opportunities and prospects in the chemical recycling of carbon dioxide to fuels., *Catalysis Today*, Vol. 148, pp. 191–205, 2009.
[5] Yu K.M.K., Curcic I., Gabriel J., and Tsang S.C.E., Recent advances in CO_2 capture and utilization., *ChemSusChem.* Vol. 1, pp. 893–899, 2008.
[6] Dry M.E., The Fischer-Tropsch process: pp. 1950-2000, 2002.

[7] Snoeckx R., Ozkan A., Reniers F., and Bogaerts A., The quest for value-added products from carbon dioxide and water in a dielectric barrier discharge: A chemical kinetics study., *ChemSusChem,* Vol. 10, pp. 409–424, 2017.
[8] Kwak H.S., Uhm H.S., Hong Y.C., and Choi E.H., Disintegration of carbon dioxide molecules in a microwave plasma torch, *Sci. Rep.*, Vol. 5, 18436, 2015.
[9] Snoeckx R. and Bogaert A. s, Plasma technology-a novel solution for CO_2 conversion., *Chem. Soc. Rev.,* Vol. 46, pp. 5805–5863, 2017.
[10] Fridman A.A., Plasma chemistry, *Cambridge University Press*, 2008.
[11] Yin Y., Yan T.g, Li Z., Devid E., Auerbach D., Kleyn A.W., CO_2 conversion by plasma: how to get efficient CO_2 conversion and high energy efficiency., *Phys. Chem. Chem. Phys.*, Vol. 23, pp. 7974–7987, 2021.
[12] Bogaerts A. and G. Centi, Plasma Technology for CO_2 Conversion: A personal perspective on prospects and gaps., *Front. Energy Res.*, Vol. 8, 111, 2020.
[13] Paulussen S., Verheyde B., Tu X., Bie C. de, Martens T., Petrovic D., Bogaerts A., and Sels B., Conversion of carbon dioxide to value-added chemicals in atmospheric pressure dielectric barrier discharges., *Plasma Sources Sci. Technol.*, Vol. 19 (3), 034015, 2010.
[14] Aerts R., Somers W., AND Bogaert A.s, Carbon dioxide splitting in a dielectric barrier discharge plasma: A combined experimental and computational study, *ChemSusChem*., Vol. 8, pp. 702–716, 2015.
[15] Mei D., He Y.L., Liu S., Yan J., and Tu X., Optimization of CO_2 conversion in a cylindrical dielectric barrier discharge reactor using design of experiments, *Plasma Proc. Polym.*, Vol. 13, pp. 544–556, 2016.
[16] Ozkan A., Dufour T., Silva T., Britun N., Snyders R., Bogaerts A., and Reniers F., The influence of power and frequency on the filamentary behavior of a flowing DBD - Application to the splitting of CO_2, *Plasma Sources Sci. Technol.*, Vol. 25 (2), 025013, 2016.
[17] Lindon M.A., Scime E.E., CO_2 dissociation using the Versatile atmospheric dielectric barrier discharge experiment (VADER), *Frontiers in Physics*, Vol. 2, pp. 1–13, 2014.
[18] Ray D., Subrahmanyam C., CO_2 decomposition in a packed DBD plasma reactor: Influence of packing materials, *RSC Adv.*, Vol. 6, pp. 39492–39499, 2016.
[19] Laer K. van, and Bogaerts A., Improving the conversion and energy efficiency of carbon dioxide splitting in a zirconia-packed dielectric barrier discharge reactor, *Energy Technol.,* Vol. 3, pp. 1038–1044, 2015.
[20] Indarto A., Yang D.R., Choi J.W., Lee H., Song H.K., Gliding arc plasma processing of CO_2 conversion, *J. Haz. Mat.*, Vol. 146, pp. 309–315, 2007.
[21] Nunnally T., Gutsol K., Rabinovich A., Fridma A.n, Gutsol A., Kemoun A., Dissociation of CO_2 in a low current gliding arc plasmatron., *J. Phys. D: Appl. Phys.*, Vol. 44 (27), 274009, 2011.
[22] Horvath G., Skalny J.D., and Mason N.J., FTIR study of decomposition of carbon dioxide in dc corona discharges, *J. Phys. D: Appl. Phys*, Vol. 41 (22), 225207, 2008.
[23] Uhm H.S., Kwak H.S., and Hong Y.C., Carbon dioxide elimination and regeneration of resources in a microwave plasma torch, *Environ. Pollut.*, Vol. 211, pp. 191–197, 2016.
[24] Chen G., Georgieva V., Godfroid T., Snyders R., and Delplancke-Ogletree M.P., Plasma assisted catalytic decomposition of CO_2, *Appl. Cat. B: Environ.*, Vol. 190, pp. 115–124, 2016.
[25] Reyes P.G., Mendez E.F., Osorio-Gonzalez D., Castillo F., and Martínez H., Optical emission spectroscopy of CO_2 glow discharge at low pressure, *Physica Status Solidi (C)*, pp. 907–910, 2008.
[26] Kogelschatz U., Dielectric-barrier Discharges: Their History, Discharge Physics, and Industrial Applications., *Plasma Chem. Plasma Proc.*, Vol. 23, pp. 1–46, 2003.
[27] Yu Q., Kong M., Liu T., Fei J., Zheng X., Characteristics of the decomposition of CO_2 in a dielectric packed-bed plasma reactor, *Plasma Chemistry and Plasma Processing*, Vol. 32, pp. 153–163, 2012.
[28] Duan X., Li Y., Ge W., and Wang B., Degradation of CO_2 through dielectric barrier discharge microplasma, *Greenhouse Gases: Sci. Technol.*, Vol. 5, pp. 131–140, 2015.
[29] Ozkan A., Dufour T., Bogaerts A., and Reniers F., How do the barrier thickness and dielectric material influence the filamentary mode and CO_2 conversion in a flowing DBD, *Plasma Sources Sci. Technol.,* Vol. 25 (4), 045016, 2016.
[30] Alliati M., Mei D., and Tu X., Plasma activation of CO_2 in a dielectric barrier discharge: A chemical kinetic model from the microdischarge to the reactor scales, *J.* CO_2 *Util.*, Vol. 27, pp. 308–319, 2018.
[31] Mei D., and Tu X., Conversion of CO_2 in a cylindrical dielectric barrier discharge reactor: Effects of plasma processing parameters and reactor design, *J.* CO_2 *Util.,* Vol. 19 pp. 68–78, 2017.
[32] Uytdenhouwen Y., Alphen S. van, Michielsen I., Meynen V., Cool P., and Bogaerts A., A packed-bed DBD micro plasma reactor for CO_2 dissociation: Does size matter, *Chem. Eng. J,* Vol. 348, pp. 557–568, 2018.
[33] Younas M., Shafique S., Faisa A.l, Hafeez A., Javed F., Mustafa M., and Rehman F., Hydrogen production through water vapors using optimized corona-DBD hybrid plasma micro-reactor, *Fuel*, Vol.331 (2), 125838, 2023.
[34] Wang B., Yan W., Ge W., and Duan X., Methane conversion into higher hydrocarbons with dielectric barrier discharge micro-plasma reactor, *J. Energy Chem.*, Vol. 22 (6), pp. 876–882, 2013
[35] Vermeiren V., and Bogaerts A., Improving the energy efficiency of CO_2 conversion in nonequilibrium plasmas through pulsing, *J. Phys. Chem.* (C), Vol. 123, pp. 17650–17665, 2019.

[36] Montesano C., Quercetti S., Martini L.M., Dilecce G., and Tosi P., The effect of different pulse patterns on the plasma reduction of CO_2 for a nanosecond discharge, *J.* CO_2 *Util.*, Vol. 39, 101157, 2020.
[37] Adrianto D., Sheng Z., Nozaki T., Mechanistic study on nonthermal plasma conversion of CO_2, *Int. J. Plasma Environ. Sci. Technol.* Vol.14 (1), e01003, 2020.
[38] Pinhão N., Moura A., Branco J.B., and Neves J., Influence of gas expansion on process parameters in non-thermal plasma plug-flow reactors: A study applied to dry reforming of methane, *Int. J. Hydrogen Energy*, Vol. 41, pp. 9245–9255, 2016.
[39] Motret O., Hibert C., Pellerin S., and Pouvesle J.M., Rotational temperature measurements in atmospheric pulsed dielectric barrier discharge-gas temperature and molecular fraction effects, *J. Phys. D: Appl. Phys.*, Vol. 33 (12), pp. 1493–1498, 2000.
[40] Manley T, The electric characteristics of the ozonator discharge, *Trans. Electrochem. Soc.*, Vol. 84, pp. 83–96, 1943.
[41] Pipa A. v., Hoder T., and Brandenburg R., On the role of capacitance determination accuracy for the electrical characterization of pulsed driven dielectric barrier discharges, *Contrib. Plasma Phys.*, Vol. 53, pp. 469–480, 2013.
[42] Pipa A. v. and Brandenburg R., The equivalent circuit approach for the electrical diagnostics of dielectric barrier discharges: The classical theory and recent developments, *Atoms*, Vol. 7 (1), 14, 2019.
[43] Mei D., Zhu X., He Y.L., Yan J.D., and Tu X., Plasma-assisted conversion of CO_2 in a dielectric barrier discharge reactor: Understanding the effect of packing materials, *Plasma Sources Sci. Technol.*, Vol. 24 (1), 015011, 2015.
[44] Zhao G.B., Argyle M.D., and Radosz M., Effect of CO on NO and N_2O conversions in nonthermal argon plasma, *J. Appl. Phys.*, Vol. 99 (11), 113302, 2006.
[45] Zhang K., and Harvey A.P., CO_2 decomposition to CO in the presence of up to 50% O_2 using a non-thermal plasma at atmospheric temperature and pressure, *Chem. Eng. J.,* Vol. 405, 126625, 2021.
[46] Li R., Tang Q., Yin S., Sato T., Investigation of dielectric barrier discharge dependence on permittivity of barrier materials, *Appl. Phys. Lett.*, Vol. 90 (13), 131502, 2007.
[47] Li J., Zhu S., Lu K., Ma C., Yang D., and Yu F., CO_2 conversion in a coaxial dielectric barrier discharge plasma reactor in the presence of mixed ZrO_2-CeO_2, *J. Environ. Chem. Eng.*, Vol. 9 (1), 104654, 2021.
[48] Taghvaei H., Pirzadeh E., Jahanbakhsh M., Khalifeh O., and Rahimpour M.R., Polyurethane foam: A novel support for metal oxide packing used in the non-thermal plasma decomposition of CO_2, *J.* CO_2 *Util.*, Vol. 44, 101398, 2021.